Temperature Anomalies in the Olympic Coast National Marine Sanctuary and the Influence of Winds and Currents during the 2013-2014 Northeast Pacific Marine Heat Wave and 2015 El Niño

Julie Ann Koehlinger

A thesis

submitted in partial fulfillment of the

requirements for the degree of

Master of Marine Affairs

University of Washington

2018

Committee:

Terrie Klinger

Jan Newton

John Mickett

Program Authorized to Offer Degree:

School of Marine and Environmental Affairs

University of Washington

Abstract

Temperature Anomalies in the Olympic Coast National Marine Sanctuary
and the Influence of Winds and Currents
during the 2013-2014 Northeast Pacific Marine Heat Wave and 2015 El Niño

Julie Ann Koehlinger

Chair of the Supervisory Committee:

Terrie Klinger

School of Marine and Environmental Affairs

The Olympic Coast National Marine Sanctuary is located in the northeast Pacific Ocean and off the northwest coast of Washington**.** Using spring to fall water temperature records from sanctuary moorings, I constructed a climatology of this nearshore environment and examined temperature anomalies during the 2013-14 northeast Pacific marine heat wave and 2015 El Niño events. My analysis focused on assessing the spatial and temporal extent of these anomalies. I also examine the influence of winds and currents and their relationship to water temperature at the mooring sites. My results show significant positive temperature anomalies that have durations of 10-20 days and are strongly correlated with wind and current observations.

Acknowledgements

I would like to thank my thesis committee: Terrie Klinger, Jan Newton, and John Mickett for their support and feedback throughout this process. My analysis benefitted immeasurably from John's expertise and each of my committee members spent many hours helping me improve this work.

I would also like to thank the Olympic Coast National Marine Sanctuary, particularly Jenny Waddell and Kathy Hough. This thesis would not have been possible without the data from their oceanographic research program and their willingness to answer all of my questions.

My path would have been much different and more difficult without the support of so many: Patrick Corrigan, who helped me find the path to lost joy, Lynne Sailer, who allowed me incredible flexibility in my work schedule so that I could follow my heart back to school, LuAnne Thompson, who took me under her wing as an oceanography undergraduate student and set me up for success, and all of the friends who unwaveringly supported me through this graduate program.

Most importantly, I thank my son, Beldon Phelps, who willingly came along on this ride with me (even though he had no say in the matter), forgave me the time I spent studying, and still loves me unconditionally. Beldon, I'm looking forward to digging up dinosaurs with you this summer and someday reading your dissertation in paleontology.

Introduction

Globally, the upper 75m of the ocean warmed by an average of 0.11 ºC per decade from 1971-2010 (Intergovernmental Panel on Climate Change 2014). This trend is expected to continue over the majority of the World's oceans (Lima and Wethey 2012; Alexander et al. 2018).

Marine heat waves (MHW) are anomalous, large scale warm water events characterized by their intensity, duration, and spatial extent (Hobday et al. 2016; Scannell et al. 2016). These events have been observed to result in shifts in geographic species distributions and declines in species abundance. Such occurrences have been distributed across the global oceans including the Mediterranean Sea (Garrabou et al. 2009; Colloca et al. 2013), the north Atlantic (Mills et al. 2013; Chen et al. 2014), off the coast of western Australia (Pearce and Feng 2013), and the northeast Pacific (Bond et al. 2015; Cavole et al. 2016).

A MHW (popularly known as "the Blob") developed in the northeast Pacific during the fall of 2013. It persisted through 2014. Satellite sea surface temperature (SST) anomalies as much as +4 ºC were observed in the California Current (Leising et al. 2015) and offshore buoy data recorded temperature anomalies of up to +6 ºC (Mickett et al. 2015). Indicators of coastal upwelling in 2014 showed below average to average upwelling and biological productivity indicators were also lower than average (Leising et al. 2015; Moore et al. 2015).

Following this MHW, a strong El Niño developed in the equatorial Pacific during 2015. The extent of its influence on water properties at the latitude of the OCNMS is not

known. Furthermore, lingering effects from the Blob versus the northward progression of the El Niño influence have not been differentiated.

Most observations of the Blob were focused on satellite or offshore buoy data, yet it is the nearshore area that is of greatest importance to numerous species of ecological, economic, and cultural importance. Marine sanctuaries established in nearshore environments help protect ecosystems from direct sources of pollution and other threats, but are still subject to climate change and extreme events. Both the gradual temperature increase predicted to occur with climate change and the shock of extreme events like marine heat waves and El Niño, along with contemporaneous stressors like eutrophication and ocean acidification, have important consequences for marine organisms, their food webs, and the socioeconomic systems of humans who depend on them (Halpern et al. 2008; Doney et al. 2011). This study examines the occurrence of positive temperature anomalies in the nearshore of the Olympic Coast National Marine Sanctuary (OCNMS).

The OCNMS is an 8257-square km marine protected area located in the northeast Pacific Ocean off the northwest coast of Washington. It spans 217 km of coastline and extends up to 80 km seaward and is fully embedded within the California Current System (CCS). The OCNMS is home to commercial, recreational, and subsistence fisheries. Four federally recognized tribes, the Makah, Quileute, Hoh, and Quinault, retain treaty rights to fish in their usual and accustomed fishing areas within the OCNMS.

The physical oceanographic characteristics of eastern boundary current systems such as the CCS are modulated by the dynamics of seasonal upwelling and downwelling. The strengthening of upwelling-favorable winds, which bring colder water to the mixed layer, may temporarily dampen the warming effects of climate change (Bakun 1990;

Sydeman et al. 2014; Bakun et al. 2015), but even this dampening effect is expected to be eventually overwhelmed by the effects of climate change (Hauri et al. 2013; Mora et al. 2013).

To examine the influence of the 2013-14 northeast Pacific marine heat wave (the Blob) and the 2015 El Niño event on nearshore temperature in the OCNMS, I constructed a baseline spring-to-fall climatology. I hypothesized that both events would be detectable in the nearshore waters as positive temperature anomalies (PTAs) but that the influence of coastal upwelling and alongshore wind stress would modulate their effect.

Methods

I used data from four OCNMS moorings located along the Washington coast (Figure 1). The Makah Bay (MB, 48.324 N 124.735 W) and Cape Alava (CA, 48.166 N 124.823 W) moorings have been deployed since 2001. A mooring at Teahwhit Head (TH, 47.876 N 124.733 W) was added in 2002, and a mooring at Cape Elizabeth (CE, 47.353 N 124.489 W) was added in 2004. All stations are within 15 km of the shoreline with bottom depths of approximately 42 m. The moorings were deployed from spring to fall each year.

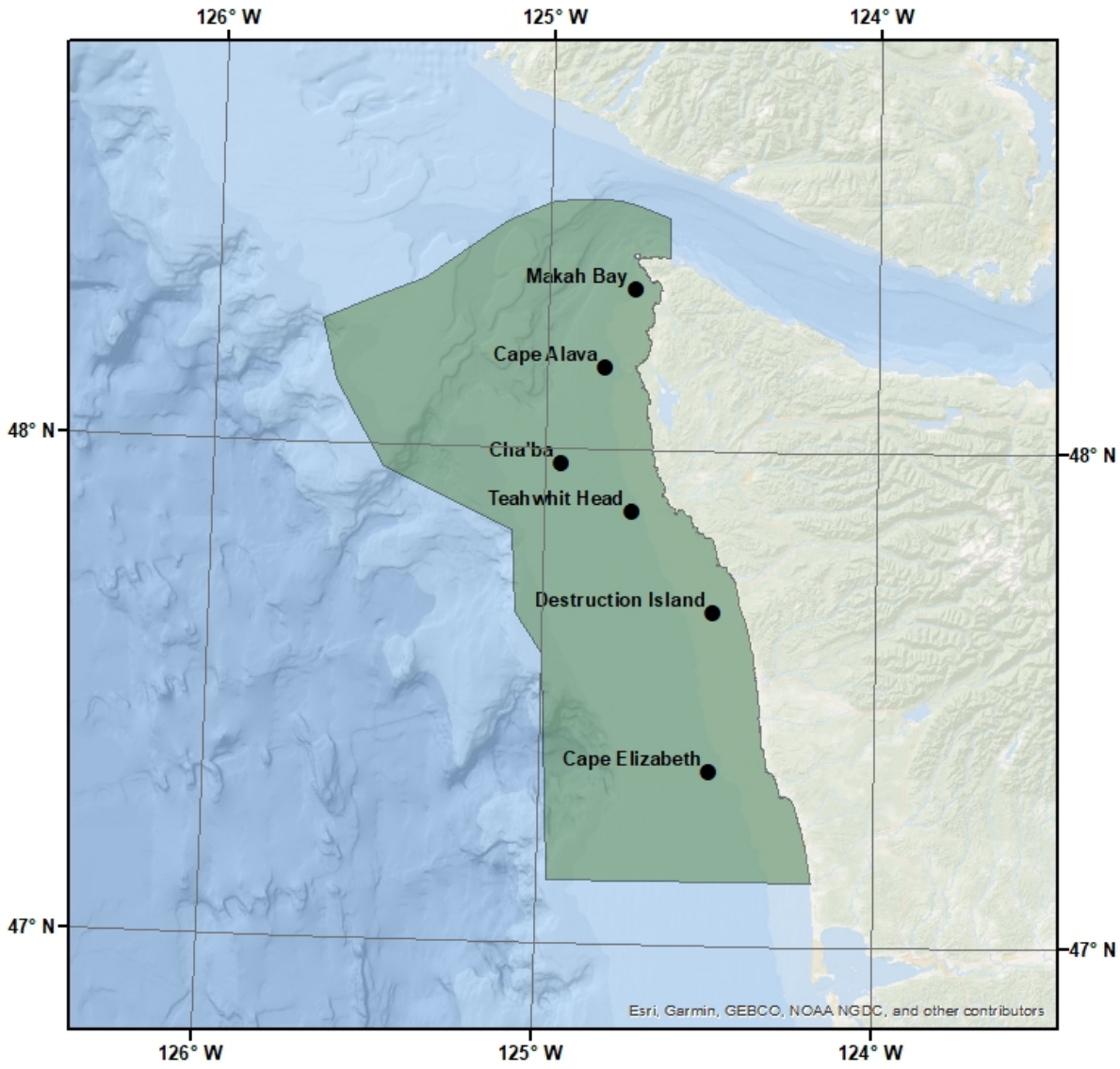

Figure 1. Mooring locations. OCNMS moorings include Makah Bay, Cape Alava, Teahwhit Head and Cape Elizabeth. The OCNMS is shaded in darker green.

The beginning and end dates for data collection varied by year and by station. For consistency, I restricted my analysis to data collected between June 1 and October 15. Equipment failure led to occasional gaps in the data and the absence of data from Teahwhit Head in the year 2011. Instrumentation varied by year and included the Onset StowAway

TidbiT Temperature Data Logger TBI-32, the Onset TidbiT v2 Water Temperature Data Logger UTBI-001, and the Sea-Bird Electronics 37-SM MicroCAT and SeaCAT 16 plus. Sampling frequency was every 2, 8, or 10 minutes. Detailed temperature instrumentation information is listed in Table 1.

Station	Years	Depths	Instrumentation	Precision
MB CA	2001-2005	40 m	TidbiT TBI-32	+/- 0.2
TH	2002-2005 2009 (5/1-7/8) 2010 (6/6-8/20)			
CE	2004-2006			
TH	2009 (7/9-10/7) 2010 (8/21-10/12)	40 m	TidbiT UTBI-001	+/- 0.02
MB CA TH CE	2013-2015	near-surface-40 m		
MB	2006-2011	40 m	SBE 37-SM MicroCAT	+/- 0.002
TH	2006			
MB	2012-2015	40 m	SBE SeaCAT 16 plus	+/- 0.002
CA	2006-2015			
TH	2007-2008 2012-2015			
CE	2007-2015			

Table 1. Instrumentation used by station, year, and depth.

I examined temperature anomalies at 40 m nominal depth by constructing climatologies for the 9-12 year period of data up to and including 2012. The analysis focused on 40 m data to examine mechanisms causing the PTAs and minimize influence from local atmospheric forcing that may affect surface values.

All temperature data were smoothed with a boxcar filter over 24 hours and then interpolated onto a daily grid. Climatology was determined by averaging daily values through 2012. Average daily values were then smoothed using a moving seven-day average. Yearly data (at nominal depths ranging from 1-40 m) from 2013, 2014, and 2015 at each station were also smoothed using a moving seven-day average. I derived temperature anomalies for the years 2013-2015 by subtracting the climatology from the absolute temperatures.

To evaluate the influence of local winds, I used wind data from NOAA's NBDC Destruction Island Station (Station DESW1 at 47.675 N 124.485 W, Figure 1) for the period June 1-October 15 in 2014 and 2015. Sampling frequency of wind data was every 60 minutes. Wind direction was rotated 15 degrees counterclockwise and the alongshore northward component of wind stress was calculated using Large and Pond's (1981) drag formula. Wind stress was smoothed with a boxcar filter over 24 hours, interpolated onto a daily grid, and then smoothed with a moving seven-day average. I then calculated correlation coefficients between northward wind stress and the change in daily average temperature at each station.

I used current data from the Northwest Association of Networked Ocean Observing Systems (NANOOS) / University of Washington Applied Physics Lab's (UW-APL) Cha'Ba buoy off of La Push, Washington (47.97 N 124.95 W, Figure 1) to further investigate mechanisms driving temperature variations. Current data from August 2 – October 7, 2014 was obtained from a 300 kHz upward-facing acoustic doppler current profiler (ADCP) deployed at a nominal depth of 90 m. Water profiling pings every 25 seconds were averaged into 10 minute ensembles at 2 m depth intervals. Current data from June 25 –

September 21, 2014 and May 23 – October 22, 2015 was obtained from a 600 kHz upward-facing ADCP at a nominal depth of 15 m. Ten 1-second water profiling pings were averaged into 2 minute ensembles at 0.5 m depth intervals, and subsampled every 10 minutes. I used average current data from 8-10 m. Data from both years was smoothed over 24 hours with a boxcar filter, and interpolated onto a daily grid. It was then smoothed with a moving 7-day average for comparison with wind data.

Results

Both the climatology and 2013-2015 record showed seasonal patterns while 2013-2015 also showed distinct variation in the form of large positive temperature anomalies that were most evident during the late summer/early fall.

2001-2012 Climatology

I observed a seasonal pattern of warm (spring) - cool (summer) - warm (fall) temperatures at all four stations. The maximum temperature peak in the June 1 to October 15 period occurred after October 1, and late summer/early fall temperatures had greater variability in their range compared to spring and summer (Figure 2). Minimum temperatures were similar across the four stations (7.3-7.4 ^{o}C), with a slightly larger range in maximum temperature (9.4-10.1 ^{o}C) (Table 2). From MB to TH the maximum temperature increased from north to south. The exception to this was CE, the southernmost station, which was colder than any of the other stations.

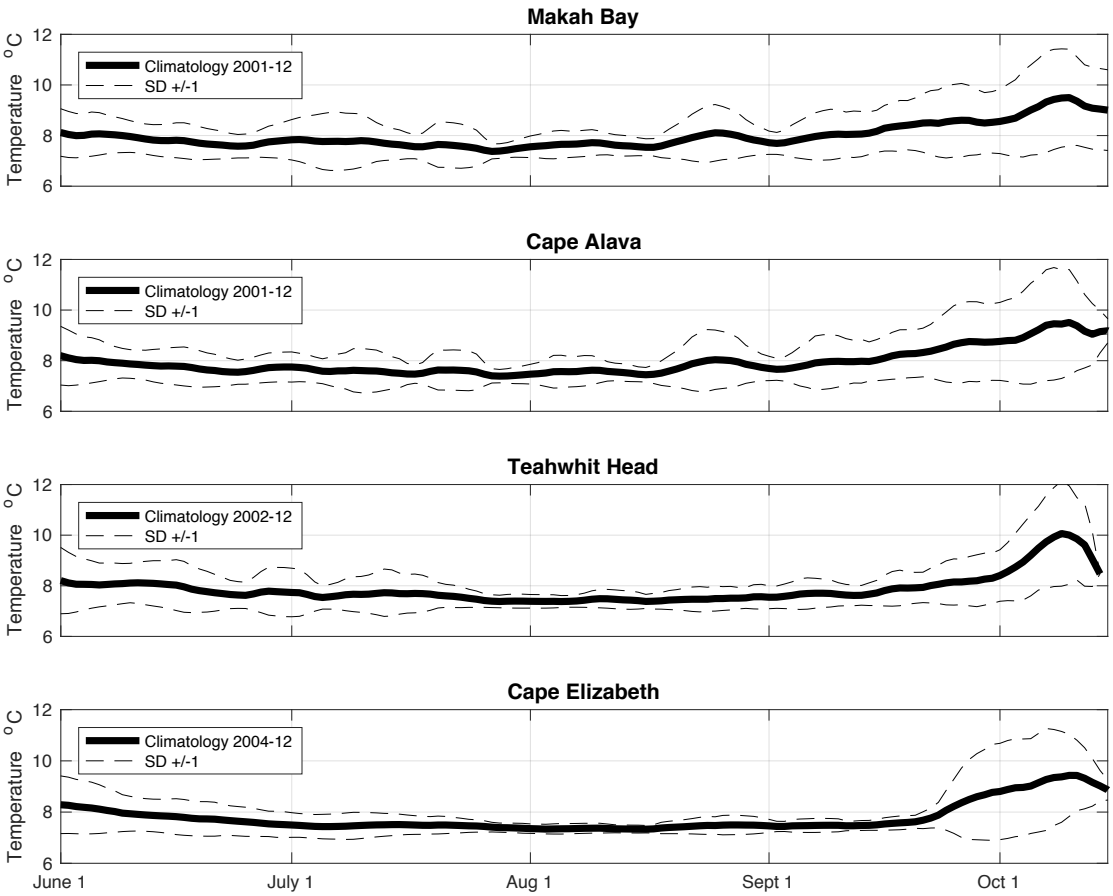

Figure 2. Climatology at each of the four stations (solid black line) with +/- one standard deviation (dashed lines).

Station (years of climatology)	Minimum (ºC)	Maximum (ºC)
Makah Bay (2001-12)	7.4 +/- 0.3	9.5 +/- 1.9
Cape Alava (2001-12)	7.4 +/- 0.3	9.7 +/- 2.1
Teahwhit Head (2002-12)	7.4 +/- 0.2	10.1 +/- 2.1
Cape Elizabeth (2004-12)	7.3 +/- 0.1	9.4 +/- 1.6

Table 2. Minimum and maximum temperatures in degrees Celsius at each station with +/- 1 standard deviation. Stations are listed in order from north to south. Initial year of data collection varies as noted.

2013-2015 Temperature Anomalies

The 2013-2015 temperature records differed from the climatology by showing distinct pulses of higher temperatures at MB, CA, and TH. Moreover, the maximum temperature was *highest* at MB and *decreased* from north to south. In most cases there was a north-south gradient in the magnitude of the PTAs, with the largest PTAs in the north at MB and the smallest in the south at CE (Table 3).

Station	2013			2014	2015		
	Jun	Aug-Sept	Oct	Sept	July	Early Sep	Late Sep
Makah Bay							
Max Temp (ºC)	9.0	10.9	13.0	12.1	9.7	11.7	10.6
Max Anomaly (ºC)	1.4	3.2	4.5	3.5	2.0	4.0	2.2
Std dev (σ) above climatology	2	6	3	2	3	9	2
Cape Alava							
Max Temp (ºC)	8.4	9.4	12.5	10.9	8.7	11.6	9.5
Max Anomaly (ºC)	0.7	1.7	3.7	2.3	1.1	3.9	1.3
Std dev (σ) above climatology	1	3	2	1	2	9	1
Teahwhit Head							
Max Temp (ºC)	8.0	8.4	12.6	9.9	8.3	11.3	9.5
Max Anomaly (ºC)	0.3	0.9	4.0	1.7	0.6	3.8	1.6
Std dev (σ) above climatology	<1	2	3	1	<1	8	2
Cape Elizabeth							
Max Temp (ºC)	7.8	7.5	8.4	9.6	7.8	no data	no data
Max Anomaly (ºC)	0.3	<0.1	0.4	1.0	0.1	n/a	n/a
Std dev (σ) above climatology	<1	<1	1	<1	<1	n/a	n/a

Table 3. Maximum temperature and maximum temperature anomaly (ºC) and number of standard deviations above climatology at each station during peak temperature anomaly periods.

These PTA pulses were seen throughout the record (Figure 3). The magnitude of the anomalies was smallest in June/July and largest in September/October. The duration of the PTA pulses typically lasted from about ten days to two weeks, with the exception of the last

2013 pulse (in October), which lasted about twenty days and was also marked with the highest peak temperature anomaly, 4.5 ºC at MB (Figure 4 a, b, c).

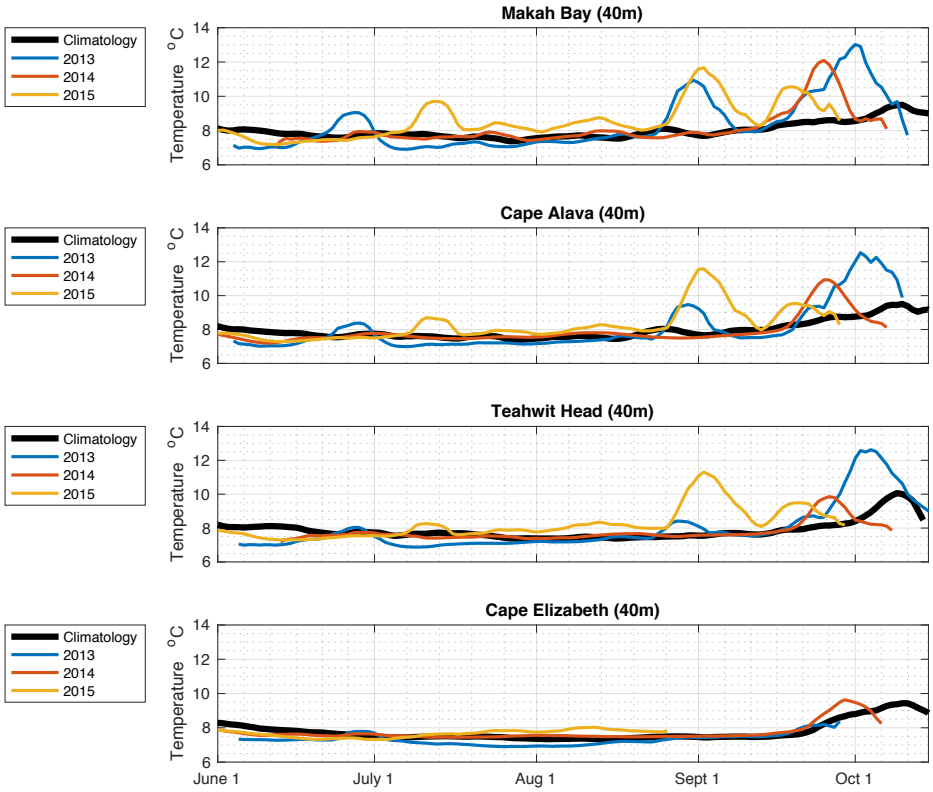

Figure 3. Observed 40 m temperatures at each station in 2013 (blue line), 2014, (orange line), and 2015 (yellow line). Climatology at each station (black line) given as a reference.

In 2013, I observed PTAs peaking in June, late August/early September, and October. The temperature anomalies of these pulses peaked at 4.5ºC in October at Makah Bay and formed a north-south gradient in June and August/September. In October, anomalies were largest at Makah Bay, while anomalies at Teahwhit Head were slightly

(0.3 ºC) larger than at Cape Alava. Cape Elizabeth, the southernmost station, remained within +/- 1σ of its baseline climatology (Table 3, Figure 4a).

In 2014, temperatures remained within +/- 1σ of climatology at all stations until late September. PTAs showed the same pattern as the June and late August/early September anomalies of 2013. The largest anomaly (3.5 ºC) was at Makah Bay in the north and there was again a north-south gradient with only a +1 ºC (<1σ) anomaly at Cape Elizabeth (Table 3, Figure 4b).

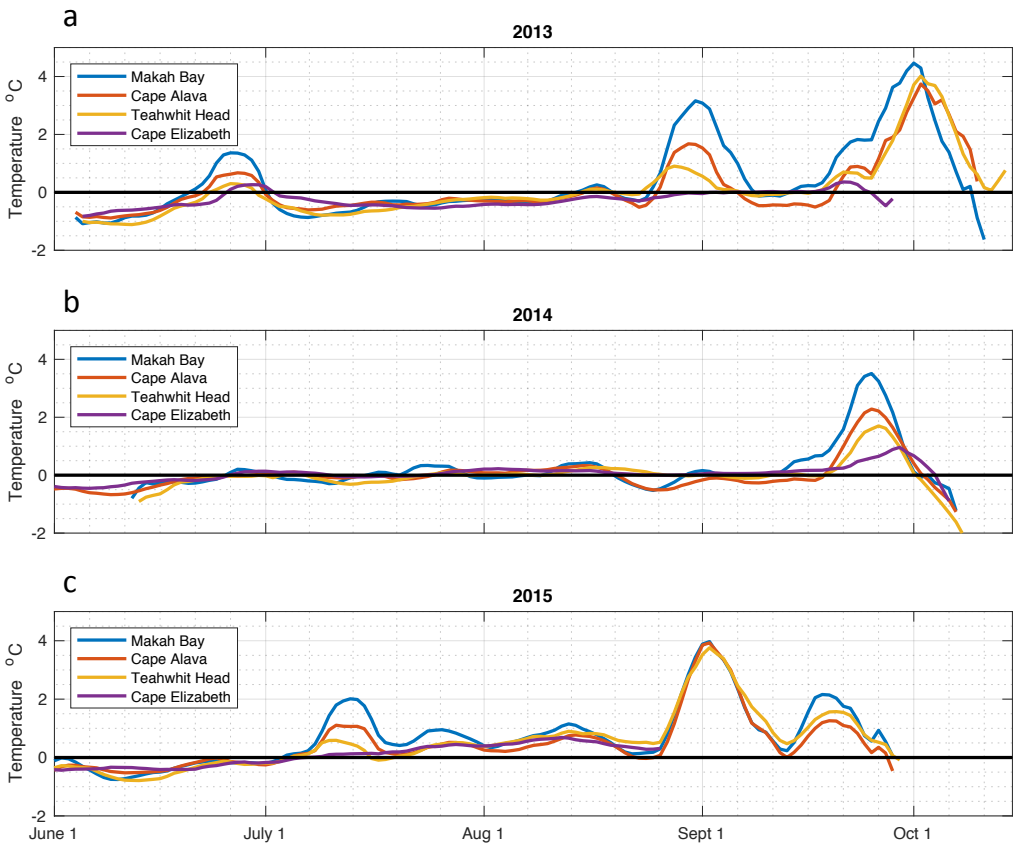

Figure 4. Temperature anomalies (ºC) at each of the four stations in (a) 2013 (b) 2014 and (c) 2015.

Three positive anomaly peaks were observed in 2015. These occurred in July and twice in September. The July and second September peak followed the pattern described above. The first September peak, however, was of similar magnitude (3.8-4.0 ^{o}C) at all stations except Cape Elizabeth, for which no data were available after mid-August (Table 3, Figure 4c).

Vertical Extent

PTAs were observed throughout the water column as shown by data taken from near-surface-40 m (Figures 5 and 6). The dynamics and timing of the PTA varied with depth. Generally, changes in temperature nearer to the surface lagged changes in temperature at depth, although this is not always the case.

In 2014, the 20, 30, and 40 m temperatures peaked at around the same time and then began to decline while the near-surface, 5 m, and 10 m temperatures continued to increase and then level off for another week before beginning to decline. This pattern was observed at all stations except Cape Elizabeth, where only the 40 m temperature record shows an earlier peak and decline (Figure 5).

In the early September pulse of 2015, the 30 and 40 m depths at Makah Bay and Cape Alava reached their peak and then began cooling first. Cooling moved upward through the water column with about a 2-day lag between each 10 m of depth. Teahwhit Head showed the same lag from 30 and 40 to 20 m (2 days), whereas the 5 m and near-surface depths lag the 20m depth by about 5 days. No data were available for Cape Elizabeth beyond August 25 (Figure 6).

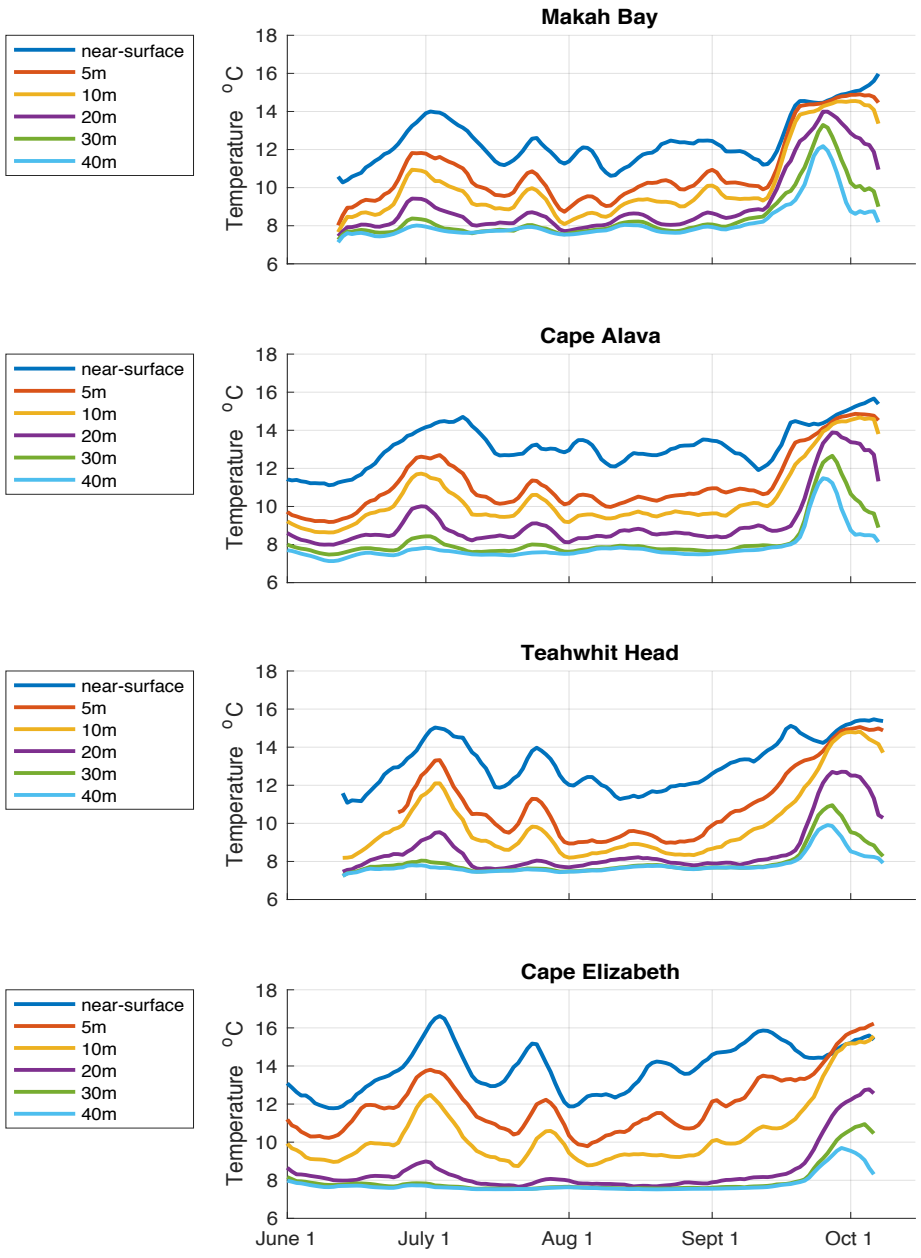

Figure 5. Temperature record (ºC) through the water column at each station in 2014.

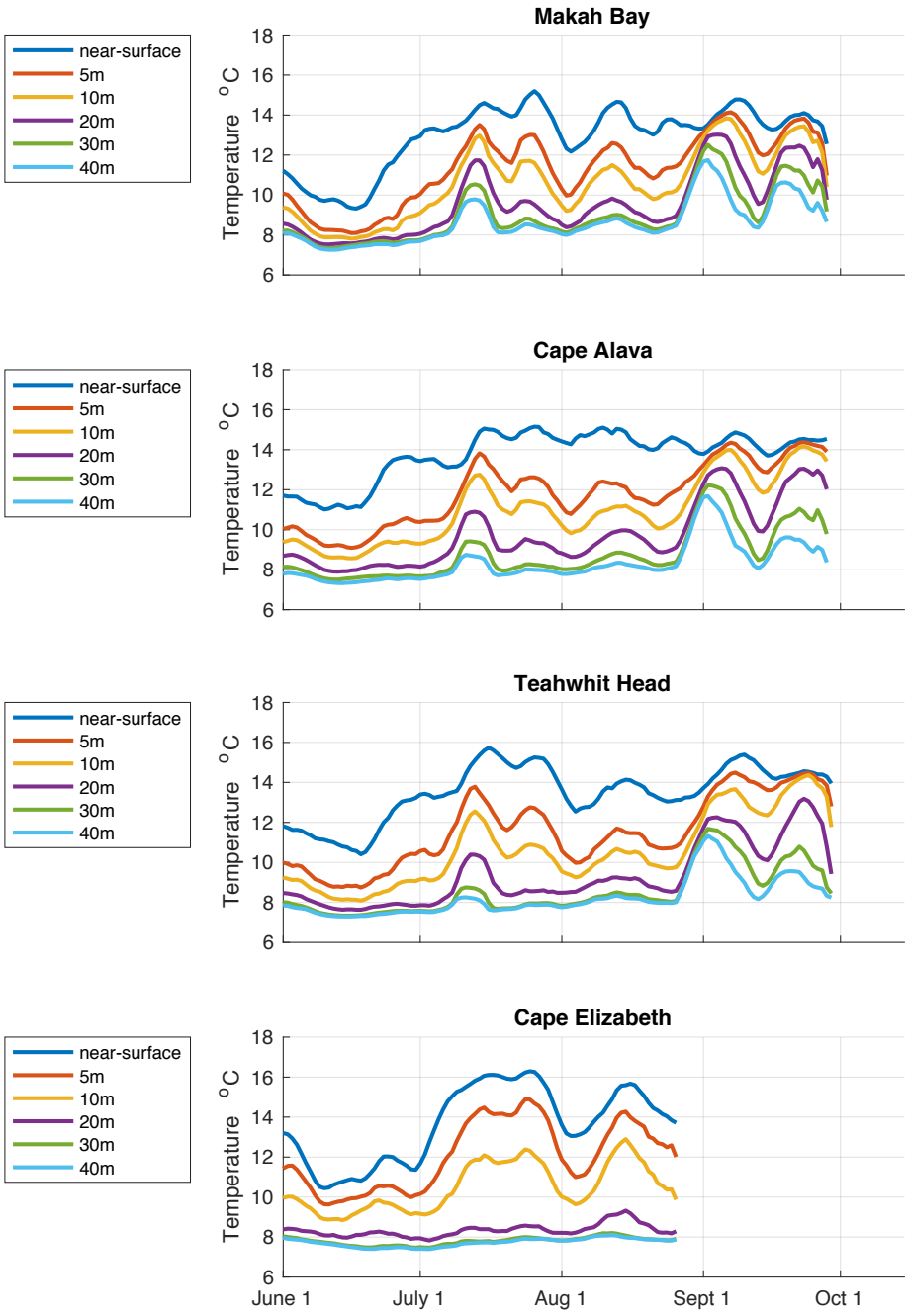

Figure 6. Temperature record (ºC) through the water column at each station in 2015.

The onset of warming in the late September pulse began at 40m across all stations and spread throughout the water column over 1-2 days, except at the Makah Bay and Teahwhit Head subsurface moorings, which lagged the other depths by an additional 2 days. Cooling occurred much more rapidly through the water column in this pulse, beginning at 30-40m and reaching the near-surface within 2-3 days (Figure 6).

Controlling Mechanisms

The mechanisms controlling PTAs were further investigated by analysis of the winds and currents. Because alongshore wind stress is an important driving force of coastal dynamics, I looked at winds from Destruction Island to determine the relationship of southerly winds to the PTAs in 2014 (Figure 7a) and 2015 (Figure 7b). I found that downwelling-favorable conditions (positive northward wind stress) occurred at the same time as pulses of increased temperature, with strong correlations in both 2014 (r = 0.38-0.49) and 2015 (r = 0.57-0.60) (Table 4). Current records from Cha'Ba also track closely with alongshore wind stress (Figure 8).

Station	2014 Correlation Coefficient	2015 Correlation Coefficient
Makah Bay	0.38	0.60
Cape Alava	0.47	0.61
Teahwhit Head	0.49	0.61
Cape Elizabeth	0.46	0.57

Table 4. Correlations between northward wind stress from Cape Elizabeth and daily change in temperature at each station.

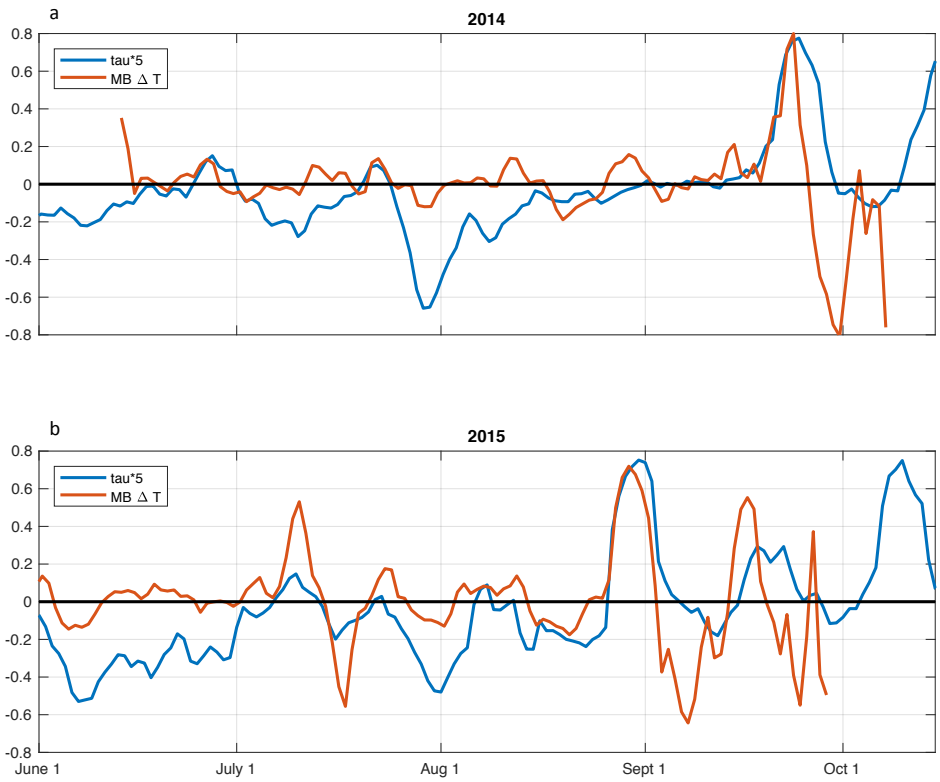

Figure 7. Alongshore wind stress at Destruction Island (blue line, multiplied by 5 for better visualization) and change in temperature at MB (orange line) in (a) 2014 and (b) 2015. Positive (negative) values indicate northward (southward) wind stress.

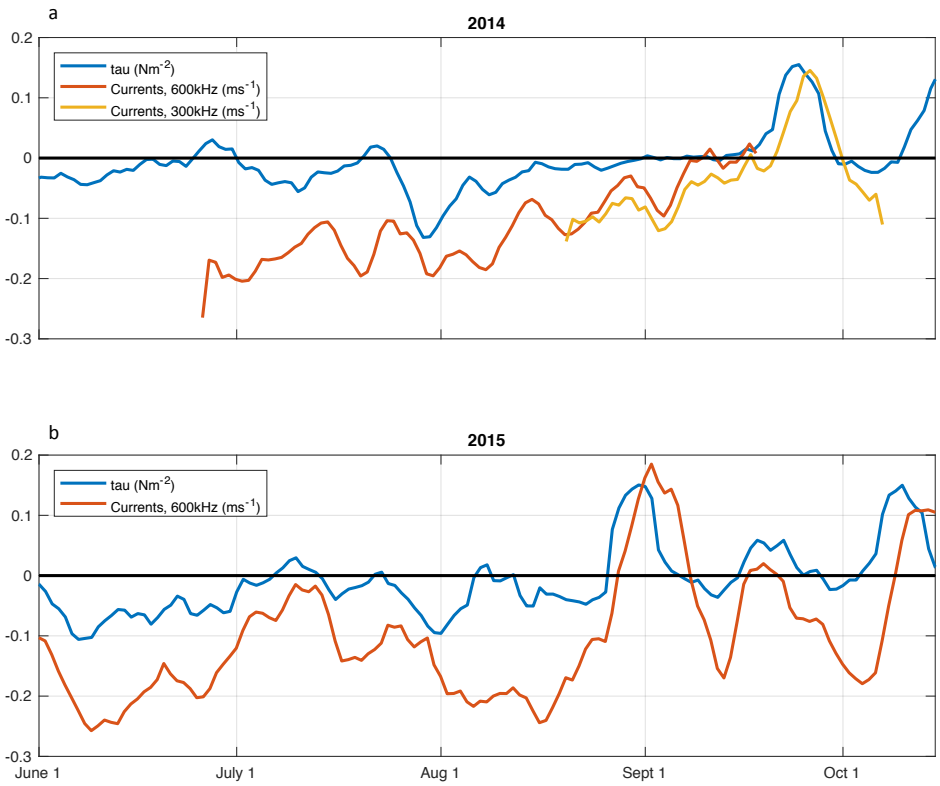

Figure 8. Wind stress (Nm^{-2}) at Destruction Island (blue line) and averaged 8-10 m currents (ms^{-1}) at Cha'Ba (orange and yellow lines) in (a) 2014 and (b) 2015. Positive (negative) values indicate northward (southward) wind stress and current flow. Current data from 2014 taken from 600 kHz ADCP (orange line) and 300 kHz ADCP (yellow line).

Discussion

I expected the temperature climatology in OCNMS to be dominated by the seasonal patterns of wind driven upwelling and downwelling . While the spring transition along the Washington coast occurs, on average, on April 29 (+/- 29 days) (Bograd et al. 2009), and is thus not captured in this data series, the late season climatologic pattern of increased variance is consistent with yearly observations of the fall transition and an average fall transition date of September 26 (+/- 20 days) (Bograd et al. 2009).

I found that the magnitude of the spring-to-fall climatologic temperature range was 2-3ºC, yet the PTAs during 2013-2015 were as high as 4.5 ºC, and occurred over a duration of 10-20 days. Such a large signal warrants further examination regarding the spatial definition of the PTAs: north to south along the coast, shallow to deep within the water column, and inshore to offshore. Here I further resolve the spatial extent of the PTAs and examine potential forcing mechanisms to elucidate the possible cause for this large signal.

By calculating Ekman transport (Q, in m^2s^{-1}) based on wind stress, I can estimate the movement of wind forced water in the offshore (onshore) direction due to upwelling (downwelling) winds:

$$Q = \tau / f\rho$$

(where τ is the northward component of wind stress, f is the Coriolis frequency and ρ is the average density at CE). The transport, Q, is 90 degrees to the right of the wind stress direction. Using estimated Ekman depths of 20, 30, and 40 m and integrating over time, I found that in 2014 water moved an estimated distance of approximately 50-100 km offshore between mid-May and mid-September, at which point there was movement back onshore (Figure 9a). The PTA seen in September of 2014 occurred when winds became downwelling-favorable and the direction of Ekman transport changed from offshore to onshore (Figure 8a and 9a). I hypothesize that downwelling-favorable conditions allowed warmer water, which had previously been kept offshore by Ekman transport associated with upwelling conditions, to move in the onshore direction and thus reach the nearshore.

In 2015, using the same estimated Ekman depths, water moved a distance of approximately 75-150 km offshore between May and late August (Figure 9b). Transport peaked in late August, just before the first September PTA in 2015, when there was again a

change to downwelling-favorable winds and the direction of Ekman transport changed from offshore to onshore (Figure 8b and 9b).

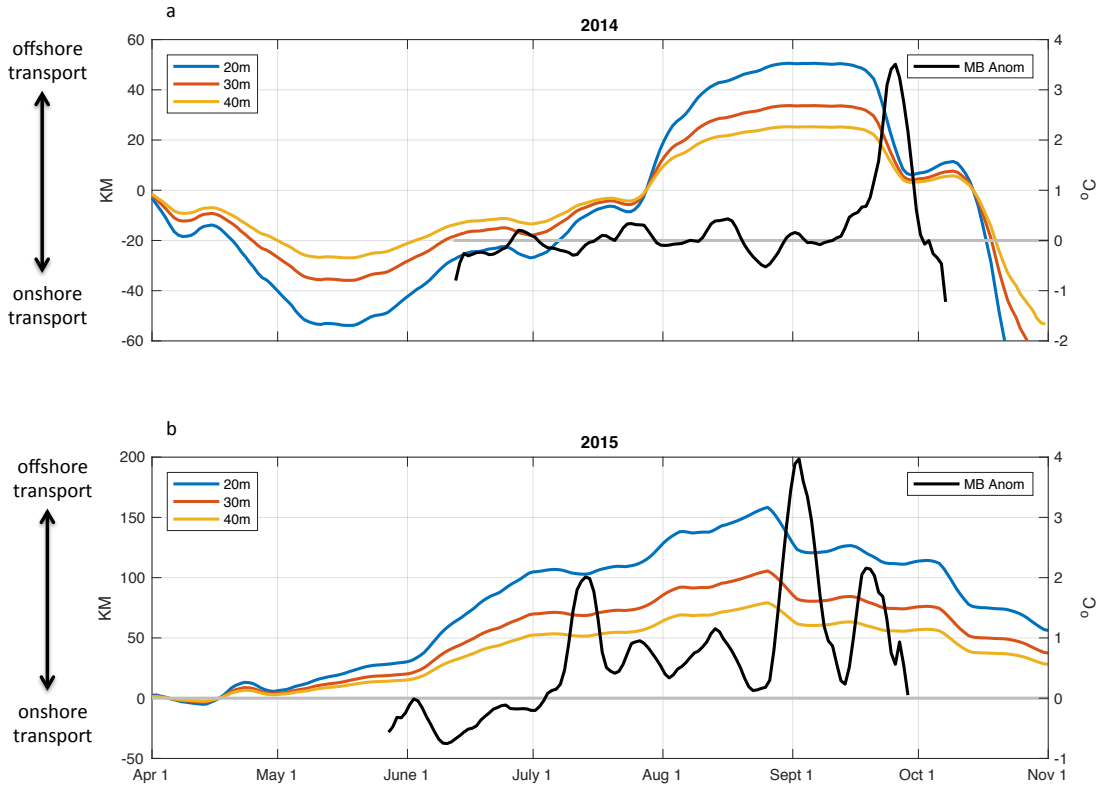

Figure 9. Estimated Ekman transport using Ekman depths of 20 m (blue line), 30 m (orange line), and 40 m (yellow line) in (a) 2014 and (b) 2015. Ekman transport in a positive direction indicates offshore transport, while transport in a negative direction indicates onshore transport. MB temperature anomalies are also plotted (black line, right sided y-axis).

The correlation of PTAs with downwelling-favorable winds and observations of northward current flow further support the advection of warmer water onshore to reach the nearshore. It is consistent that the advection of an offshore water mass of uniform

alongshore temperature into the nearshore would result in larger anomalies in the north, given the north-to-south gradient of increasing temperatures in the climatology.

However, in 2013-2015 observations I not only detected a gradient of larger anomalies from north to south, but also a reversal of the north to south absolute temperature gradient. That is, temperatures (at 40 m depths) in the north were warmer than temperatures in the south and consistently decreased from MB to CE.

With the relaxation of downwelling-favorable winds and decrease in velocity of northward current flow, cooling through the water column returned and temperature anomalies at all stations returned to within +/- 1 ^{o}C of the climatology until the next PTA event. Temperature changes nearer to the surface generally lagged temperature changes at depth. It is possible that the deeper waters are more influenced by upwelling conditions and more likely to show response to warming when this flow stops. This deeper water is then replaced by warmer water downwelling from near the coast.

Limited inshore/offshore comparisons can be made with temperature data from NANOOS/UW-APL's Cha'Ba mooring. In 2013, Cha'Ba recorded near-surface (3m) temperature warming events in early July and early September (Mickett et al. 2014), timing that is similar to the observations from the OCNMS stations. The record, however, does not extend long enough to compare with the late September PTAs in OCNMS. In 2014 Cha'Ba data show a fall warming event, but unlike the OCNMS moorings, which show significant PTAs in late September, Cha'Ba temperature data don't show warming below 40 m until well into October (Mickett et al. 2015). In 2015, Cha'Ba records higher temperatures (at 85 m) than in previous years, but temperatures remain below 10 ^{o}C until November (Mickett and Newton. 2016).

The nearshore stations of Makah Bay, Cape Alava, and Teahwhit Head showed shorter-timescale fluctuations in temperature than the satellite derived SST record of the Blob (typically averaged on monthly timescales). I was able to correlate these fluctuations with northward wind stress and downwelling-favorable conditions. When the Blob signal reached the nearshore, temperature anomalies were outside the climatologic variation, even when considering the fluctuation in timing of the fall transition.

Examination of temperature in the nearshore environment is important because of its implications for marine species, particularly benthic species with limited motility. A large body of research has been devoted to identifying thermal tolerances, particularly in intertidal and coastal environments (Madeira et al. 2012; Vinagre et al. 2013, 2015; Pörtner et al. 2017). Spatial and temporal heterogeneity of temperature throughout the marine environment is also significant for species migration and adaptation to climate change, with most marine species already living near the upper limit of their thermal tolerance (Sunday et al. 2012; Pinsky et al. 2013).

In addition to thermal tolerances, temperature affects the availability of dissolved oxygen in the ocean, which further constrains species survival. As temperatures increase, hypoxia tolerance decreases (Deutsch et al. 2015). Warming oceans overlaid with extreme events like the Blob compounds organism stress from both a thermal and hypoxic perspective.

Conclusion

Effects of the northeast Pacific Ocean marine heat wave were widespread over the California Current System, but spatially and temporally variable. This variability is particularly evident in the nearshore environment of the OCNMS, where temperature

fluctuated on timescales of days to weeks instead of weeks to months. Temperature was also significantly influenced by Ekman transport driven by local wind forcing and current flows. Understanding the potential effects of such events on nearshore ecosystems is vital to understanding climate change adaptation and underscores the need for continued monitoring programs like that of the OCNMS.

References

Alexander, M. A., J. D. Scott, K. D. Friedland, K. E. Mills, J. A. Nye, A. J. Pershing, and A. C. Thomas. 2018. Projected sea surface temperatures over the 21st century: Changes in the mean, variability and extremes for large marine ecosystem regions of Northern Oceans. Elem Sci Anth **6**. doi:10.1525/elementa.191

Bakun, A. 1990. Global Climate Change and Intensification of Coastal Ocean Upwelling. Science **247**: 198–201.

Bakun, A., B. A. Black, S. J. Bograd, M. García-Reyes, A. J. Miller, R. R. Rykaczewski, and W. J. Sydeman. 2015. Anticipated Effects of Climate Change on Coastal Upwelling Ecosystems. Curr. Clim. Change Rep. **1**: 85–93. doi:10.1007/s40641-015-0008-4

Bograd, S. J., I. Schroeder, N. Sarkar, X. Qiu, W. J. Sydeman, and F. B. Schwing. 2009. Phenology of coastal upwelling in the California Current. Geophys. Res. Lett. **36**. doi:10.1029/2008GL035933

Bond, N. A., M. F. Cronin, H. Freeland, and N. Mantua. 2015. Causes and impacts of the 2014 warm anomaly in the NE Pacific. Geophys. Res. Lett. **42**: 2015GL063306. doi:10.1002/2015GL063306

Cavole, L. M., A. M. Demko, R. E. Diner, and others. 2016. Biological Impacts of the 2013–2015 Warm-Water Anomaly in the Northeast Pacific: Winners, Losers, and the Future. Oceanography **29**: 273–285.

Chen, K., G. G. Gawarkiewicz, S. J. Lentz, and J. M. Bane. 2014. Diagnosing the warming of the Northeastern U.S. Coastal Ocean in 2012: A linkage between the atmospheric jet stream variability and ocean response. J. Geophys. Res. Oceans **119**: 218–227. doi:10.1002/2013JC009393

Colloca, F., M. Cardinale, F. Maynou, M. Giannoulaki, G. Scarcella, K. Jenko, J. M. Bellido, and F. Fiorentino. 2013. Rebuilding Mediterranean fisheries: a new paradigm for ecological sustainability. Fish Fish. **14**: 89–109. doi:10.1111/j.1467-2979.2011.00453.x

Garrabou, J., R. Coma, N. Bensoussan, and others. 2009. Mass mortality in Northwestern Mediterranean rocky benthic communities: effects of the 2003 heat wave. Glob. Change Biol. **15**: 1090–1103. doi:10.1111/j.1365-2486.2008.01823.x

Hauri, C., N. Gruber, M. Vogt, and others. 2013. Spatiotemporal variability and long-term trends of ocean acidification in the California Current System. Biogeosciences **10**: 193–216. doi:10.5194/bg-10-193-2013

Hobday, A. J., L. V. Alexander, S. E. Perkins, and others. 2016. A hierarchical approach to defining marine heatwaves. Prog. Oceanogr. **141**: 227–238. doi:10.1016/j.pocean.2015.12.014

Intergovernmental Panel on Climate Change, ed. 2014. Climate Change 2013 - The Physical Science Basis: Working Group I Contribution to the Fifth Assessment Report of the Intergovernmental Panel on Climate Change, Cambridge University Press.

Large, W. G., and S. Pond. 1981. Open Ocean Momentum Flux Measurements in Moderate to Strong Winds. J. Phys. Oceanogr. **11**: 324–336. doi:10.1175/1520-0485(1981)011<0324:OOMFMI>2.0.CO;2

Leising, A. W., I. D. Schroeder, S. J. Bograd, and others. 2015. State of the California Current 2014-15: Impacts of the Warm-Water "Blob." Calif. Coop. Ocean. Fish. Investig. Rep. **56**: 31–68.

Lima, F. P., and D. S. Wethey. 2012. Three decades of high-resolution coastal sea surface temperatures reveal more than warming. Nat. Commun. **3**: 704. doi:10.1038/ncomms1713

Mickett, J.B., Newton, J.A., and M. Alford. 2014. Coastal Ocean and Puget Sound Boundary Conditions: Coastal Ocean, Interannual comparison of water properties. In Moore, S. K., K. Stark, J. Bos, P. Williams, J. A. Newton, and K. Dzinbal, eds. 2014. Puget Sound marine waters: 2013 overview (p6).

Mickett, J.B., Newton, J.A., and M. Alford. 2015. Coastal Ocean and Puget Sound Boundary Conditions: NW Washington Coast Water Properties. In Moore, S. K., R. Wold, K. Stark, J. Bos, P. Williams, K. Dzinbal, C. Krembs, and J. A. Newton, eds. 2015. Puget Sound marine waters: 2014 overview (p8).

Mickett, J.B and J.A. Newton. 2015. Coastal Ocean and Puget Sound Boundary Condiditons: NW Washington Coast Water Properties. In Moore, S. K., R. Wold, K. Stark, J. Bos, P. Williams, K. Dzinbal, C. Krembs, and J. A. Newton, eds. 2016. Puget Sound marine waters: 2015 overview (pp7-8).

Mills, K. E., A. J. Pershing, C. J. Brown, and others. 2013. Fisheries Management in a Changing Climate: Lessons from the 2012 Ocean Heat Wave in the Northwest Atlantic. Oceanography **26**: 191–195.

Moore, S. K., R. Wold, K. Stark, J. Bos, P. Williams, K. Dzinbal, C. Krembs, and J. A. Newton, eds. 2015. Puget Sound marine waters: 2014 overview.

Mora, C., A. G. Frazier, R. J. Longman, and others. 2013. The projected timing of climate departure from recent variability. Nature **502**: 183–187. doi:10.1038/nature12540

Pearce, A. F., and M. Feng. 2013. The rise and fall of the “marine heat wave” off Western Australia during the summer of 2010/2011. J. Mar. Syst. **111**–**112**: 139–156. doi:10.1016/j.jmarsys.2012.10.009

Scannell, H. A., A. J. Pershing, M. A. Alexander, A. C. Thomas, and K. E. Mills. 2016. Frequency of marine heatwaves in the North Atlantic and North Pacific since 1950. Geophys. Res. Lett. **43**: 2015GL067308. doi:10.1002/2015GL067308

Sydeman, W. J., M. García-Reyes, D. S. Schoeman, R. R. Rykaczewski, S. A. Thompson, B. A. Black, and S. J. Bograd. 2014. Climate change and wind intensification in coastal upwelling ecosystems. Science **345**: 77–80. doi:10.1126/science.1251635